POLITECNICO DI TORINO
Repository ISTITUZIONALE

A simplified method for estimating Newmark displacements of mountain reservoirs

Original
A simplified method for estimating Newmark displacements of mountain reservoirs / Veylon, G.; Luu, L. H.; Mercklé, S.; Bard, P. Y.; Delvallée, A.; Carvajal, C.; Frigo, Barbara. - In: SOIL DYNAMICS AND EARTHQUAKE ENGINEERING. - ISSN 0267-7261. - ELETTRONICO. - 100:(2017), pp. 518-528. [10.1016/j.soildyn.2017.07.003]

Availability:
This version is available at: 11583/2676352 since: 2017-07-12T11:41:51Z

Publisher:
Elsevier

Published
DOI:10.1016/j.soildyn.2017.07.003

Terms of use:

This article is made available under terms and conditions as specified in the corresponding bibliographic description in the repository

Publisher copyright
Elsevier postprint/Author's Accepted Manuscript

© 2017. This manuscript version is made available under the CC-BY-NC-ND 4.0 license
http://creativecommons.org/licenses/by-nc-nd/4.0/.The final authenticated version is available online at:
http://dx.doi.org/10.1016/j.soildyn.2017.07.003

(Article begins on next page)

27 April 2024

A simplified method for estimating Newmark displacements of mountain reservoirs

G. Veylon[a,*], L.-H. Luu[a], S. Mercklé[a], P.-Y. Bard[b], A. Delvallée[a], C. Carvajal[a], B. Frigo[c]

[a] *Irstea, RECOVER, Aix-en-Provence, France*
[b] *Univ. Grenoble Alpes, ISTerre, Grenoble, France*
[c] *Politecnico di Torino, DISEG, Turin, Italy*

Abstract

In the present article we propose a new simplified method for assessing the seismic performance of large mountain reservoirs. The pseudo-empirical regression model is established on the basis of decoupled dynamic analyses performed on 7 accelerograms applied to 33 structural and geotechnical configurations. We study the influence of embankment geometries and mechanical properties on the prediction of earthquake-induced permanent displacements estimated by Newmark analyses. We also discuss the relevance of our model by carrying out comparisons with existing simplified models and with post-seismic field observations on earth dams. A regression analysis using parameters of interest provides a pseudo-empirical predictive equation to carry out rapid, preliminary assessments of the seismic performance of mountain reservoirs.

Keywords: Moutain reservoirs, Earth dams, Newmark analysis, Simplified methods, Seismic performance.

1. Introduction

Mountain reservoirs are hydraulic structures generally built in ski resorts. They are designed to store water used for the production of drinking water or artificial snow. These structures are located in mountainous areas, at altitudes between 1,200 and 2,700 m. They are often installed on steep slopes above facilities which are heavily populated during certain periods of the year. Depending on the geotechnical context, their failure can create torrential flows and, in spite of the low volumes of water stored, have disastrous consequences for public safety.

Mountain reservoirs are unique structures due to their geometry, the type of materials used in their construction, and the level of seismic risk to which they are exposed. Most mountain reservoirs are homogeneous earth dams. Their stability is validated by examining different design situations. These include seismic situations which, in the case of mountain reservoirs, are often critical design factors. Geotechnical investigations are difficult and expensive because the conditions of access to these dams are impeded by the topography of the sites and extreme climatic conditions. Moreover, the financial resources of the owners of such structures are limited, so a sismotectonic study of each site is not conceivable. Therefore there is a strong need for rapid and preliminary methods to evaluate the seismic performance of mountain reservoirs in a context where geotechnical data are scarce and the determination of specific accelerograms for each site is impractical.

The seismic performance assessment of earth dams is usually performed according to the pseudo-static approach [55]. This approach consists in analyzing the stability of a soil mass along a potential failure surface. The soil mass is subjected to horizontal destabilizing inertia forces, expressed in terms of a fraction of the acceleration of gravity (seismic coefficient k). Although some authors have developed a methodology to determine a relevant pseudo-static seismic coefficient from various seismic loading parameters and a target maximum displacement [10, 7, 42], this approach does not allow the evaluation of post-seismic permanent displacements.

Stress-deformation analyses enable conducting coupled nonlinear dynamic analyses [14, 29]. These approaches can simulate all the stages of the life of a structure (construction, impoundment, seismic loading, etc.), by taking into account the nonlinearity of constitutive laws, hydro-mechanical coupling, the effect of the loading history, etc. The main drawback of these methods stems from the practical difficulty of providing site-specific high density and high-quality data. Indeed, these approaches require extensive geotechnical and sismotectonic investigations. Therefore these methods are generally limited to the analysis of critical projects and are not adapted to the rapid or preliminary assessment of the seismic performance of small earth dams. The objective of permanent-displacement analysis methods is to bridge the gap between the simplistic pseudo-static approach and complex stress-deformation analyses. They are still commonly used to develop seismic assessment approaches applied to the cases of natural slopes [50, 33, 54] and retaining walls [15]. Permanent-displacement analysis methods were formulated on the ba-

*Corresponding Author
Email address: guillaume.veylon@irstea.fr (G. Veylon)

sis of the sliding block theory proposed by Newmark [40]. According to this theory, the potential sliding soil mass can be treated as a rigid body subjected to the action of seismic forces. Permanent displacements of the mass take place whenever the block acceleration exceeds a critical value called the yield acceleration. In "decoupled" procedures, the dynamic response of the embankment is computed separately from the sliding mass displacement. In "coupled" procedures, the dynamic response of the sliding mass is calculated simultaneously to its permanent displacement. The main advantage of permanent-displacement analyses is that they require few data and are particularly adapted to parametric studies.

Newmark displacements are calculated following a decoupled procedure in which a rigid-plastic response of the block is assumed. The decoupling hypothesis is known to be conservative, especially when the predominant frequency of the seismic excitation is close to the fundamental period of the dam [36, 20]. In contrast, the rigid block assumption is unconservative when the fundamental period of the sliding mass is close to the predominant period of the ground motion [46]. Some authors proposed a correction formula to account for the flexibility of the sliding mass after using rigid block assumptions to calculate the displacements [45]. However, the effect of the stiffness of the sliding block is believed to be of a secondary order relative to the amplification effects occurring in the embankment. Whatever the case, the Newmark displacement does not represent a realistic assessment of the deformation field within the structure. It is an index of the seismic performance of earth dams. If the predicted Newmark displacements are expected to be significant, a more refined method is warranted for further analyses.

To simplify the use of permanent displacement analysis methods, several authors developed empirical relationships on the basis of regression analyses performed on the basis of rigorous Newmark analysis results [38]. They proposed models that predict the Newmark displacement as function of structural parameters (yield acceleration k_y, first fundamental period of the dam T_1), ground motion parameters (peak ground acceleration PGA, earthquake magnitude M, Arias intensity I_a, predominant period of the acceleration spectrum T_m, spectral acceleration at a degraded period $S_a(1.5T_1)$, etc.) A summary of commonly referenced methods is provided in Table 1. All these methods were based on simulated Newmark displacement data computed from a large data base of worldwide earthquake records with various magnitudes and sismotectonic contexts. The application of these methods is not straightforward as they necessitate iteration and/or preliminary analyses, such as for the determination of k_{max}.

The estimation of k_{max} has to account for amplification effects related to dams's height. The estimation of k_{max} can be deduced from charts giving k_{max} as a function of PGA, T_1 and the ratio z/H representing the maximum depth of the sliding surface (measured from the crest) and the dam's height H [2, 37]. However, it has been shown that the uncertainty on the value of the peak acceleration at the crest is of the same order of magnitude as the peak ground acceleration itself [11]. The reduction of uncertainties on the peak acceleration at the crest would require the implementation of advanced dynamic analyses and considerable computational efforts that conflict with the aim of simplified methods [8]. The procedures used for the determination of k_{max} constitute the main limitation of existing simplified methods.

Therefore there is a strong need to develop more effective and simple equations that do not integrate the parameter k_{max} and which are adapted to small earth dams ($H \leq 20\,m$). Considering that the *in situ* measurements published in the literature [53] have demonstrated that the normalization of the yield coefficient k_y by the peak ground acceleration PGA is efficient, we attempt to find a relationship in the following form:

$$\ln U^* = \mathcal{F}\left(\frac{k_y\, g}{PGA}, p_1, p_2, ...p_n\right) \tag{1}$$

where U^* is a non-dimensionalized displacement and p_i are scalar parameters of the model accessible without any additional computational effort.

In this paper, our objective is to rationalize the impact of seismic loading parameters and structure characteristics on permanent displacement estimates by employing rigorous Newmark analyses. The influence of the geometrical and geotechnical characteristics on the seismic response of the dams can be studied by conducting a parametric analysis. On the basis of 231 numerical simulations, we propose a simplified model for estimating the Newmark displacements as a function of various geotechnical and seismological parameters and discuss its predictive capacity on the basis of a comparison with existing methods and *in situ* measurements published in the literature.

2. Methodology and input data

2.1. Mountain reservoirs characteristics

Generally installed in flat areas, mountain reservoirs are built by excavation and fill and founded on bedrock. In the Alps, they consist of moraines and shales and, to a lesser extent, silts or materials obtained from crushing quartzite, gneiss and limestone. The embankment is then rendered impervious by the installation of a geomembrane. The storage volume of these mountain reservoirs varies from ten thousand to several hundred thousand cubic meters.

The typical geometry of mountain reservoirs is characterized by a trapezoidal cross-section, a crest 4 meters in width, a height varying from 10 to 20 meters, and a slope ranging from $\tan\beta = 1/2$ to $\tan\beta = 1/3$. The geotechnical parameters commonly encountered in such hydraulic structures are [43]: a moist unit weight around 20 kN/m^3, an effective cohesion c' between 0 and 10 kPa, an internal friction angle ϕ' between 25^o and 35^o for a maximum shear modulus G_{max} ranging between 180 and 500 MPa.

Model	Functional form
Sarma [48]*	$\log[\frac{4U}{Ck_{max}gT_m^2}] = 0.85 - 3.91\frac{k_y}{k_{max}}$
Hynes-Griffin and Franklin [25]**	$\log[U(cm)] = -0.116(\frac{k_y}{k_{max}})^4 - 0.702(\frac{k_y}{k_{max}})^3$ $-1.733(\frac{k_y}{k_{max}})^2 - 2.854(\frac{k_y}{k_{max}}) - 0.287$
Makdisi and Seed [37]	$\frac{U}{k_{max}gT_0} = f(\frac{k_y}{k_{max}})$ [chart-based mehod]
Yegian et al. [60]	$\log[\frac{U}{N_{eq}k_{max}gT_m^2}] = 0.22 - 10.12(\frac{k_y}{k_{max}})$ $+16.38(\frac{k_y}{k_{max}})^2 - 11.48(\frac{k_y}{k_{max}})^3$
Jibson [27]	$\log[U(cm)] = 0.215$ $+\log[(1-k_y/k_{max})^{2.341}(k_y/k_{max})^{-1.438}]$
Bray and Travasarou [9]	$\log[U(cm)] = -0.22 - 2.83\ln(k_y) - 0.333(\ln(k_y))^2$ $+0.566\ln(k_y)\ln(k_{max}) + 3.04\ln(k_{max})$ $-0.244(\ln(k_{max}))^2 + 0.278(M-7)$

* Funtional form presented by Cai and Bathurst [12]
** Funtional form presented by Meehan and Vahedifard [38]

Table 1: Summary of commonly referenced rigid sliding block models.

The simulations were performed considering a constant value of moist unit weight $\gamma_h = 20kN/m^3$ and for three values of maximum shear modulus G_{max}=180, 300, 500 MPa. The values of H are small enough to consider that the effect of the mean effective stress on G_{max} is of second order as regards to its the range of variation. Therefore, G_{max} is assumed to be independent from the mean effective stress. The combinations of the other parameters defining the situations are presented in Table 2.

Not every combination of parameters was considered in this study. The combinations of parameters were chosen in order to study the specific influence of each parameter on k_y and U independently of the others: the influence of c' with combinations 1-2-3, the influence of ϕ' with combinations 1-4-5, that of the embankment slope with combinations 1-6 and 5-9, and finally the influence of the embankment height H with combinations 1-7-8 and 9-10-11. No correlation between the parameters was explicitly introduced. However, in the case of the steepest slopes ($\tan\beta$=1/2), the stability of the structure was not ensured under static loading for friction angles less than or equal to 30 degrees. Nevertheless, the contributions of the various parameters were integrated in the factor of safety F and yield acceleration k_y. Our choice of parameter combinations allowed us to generate a wide range of k_y values (0.1-0.45) corresponding to a wide range of FS values (1.2-2.2) representative of the values found on existing mountain reservoirs.

2.2. Input ground motion

The use of dynamic approaches requires input ground acceleration-time histories. The determination of such data is a rather complicated process that involves a certain level of expertise and judgment. Here, we present the findings of a thorough study conducted in the framework of the RISBA project, leading to the generation of the artificial accelerograms used for our simulations [4].

The classical method of generation Gasparini and Vanmarcke [17] was amended to limit the potentially high variability of calculated displacements associated with the use of random phase synthetic accelerograms [5]. The random phase assumption was replaced by the importation of real accelerogram phases chosen to match the possible type of earthquake (in terms of magnitude, distance, site conditions, etc.).

Accelerograms were selected from the European RESORCE database [1] to ensure better matching with the characteristics of Alpine seismicity for a return period equal to 5,000 years. The selection criteria for proper accelerograms were: *i)* a Class A site in the meaning of Eurocode 8 [16] (i.e. a rock-like foundation), *ii)* a PGA of one of the horizontal components between 3 and 4.5 m/s^2, *iii)* a maginutude entre 5.5 and 6.5 and *iv)* a distance from the epicenter less than 30 km. A set of 7 accelerograms was obtained (Table 3). Each accelerogram was normalized in order to have a peak ground acceleration $PGA = 3.5\,m/s^2$.

The synthetic accelerogram response spectra are shown in Fig. 1. Although the response spectrum is the same for all accelerograms, they can be distinguished in terms

Combination	Geometry		Geotechnical parameters	
No.	H (m)	$\tan\beta$ = H/L	c' (kPa)	ϕ' (deg.)
1	20	1/3	0	25
2	20	1/3	5	25
3	20	1/3	10	25
4	20	1/3	0	30
5	20	1/3	0	35
6	20	1/2.5	0	25
7	10	1/3	0	25
8	15	1/3	0	25
9	20	1/2	0	35
10	10	1/2	0	35
11	15	1/2	0	35

Table 2: Geometric and geotechnical properties defining the 11 configurations considered in the present study.

N^o	Earthquake (place, date, Magnitude, Epicentral distance)	Record	I_a (m s^{-1})
1	South-Iceland, 17/06/2000 15:40, M=6.5, R=20 km	6756-Flagbjarnarholt	1.21
2	South-Iceland, 17/06/2000 15:40, M=6.5, R=22 km	6760-Solheimar	1.43
3	South-Iceland, 21/06/2000 00:51, M=6.4, R=17 km	6791-Solheimar	1.11
4	South-Iceland, 21/06/2000 00:51, M=6.4, R=15 km	6799-Kalfarholt	2.00
5	South-Iceland, 21/06/2000 00:51, M=6.4, R=3 km	6802-Thjorsartun	0.90
6	Umbria-Marche, 14/10/1997 15:23, M=5.6, R=9 km	14683-Borgo Cerreto-Torre	1.88
7	Olfus Island, 29/05/2008 15:45, M=6.1, R=5 km	16352-Selfoss-City Hall	1.47

Table 3: Characteristics of the real earthquake records used to generate the 7 synthetic accelerograms.

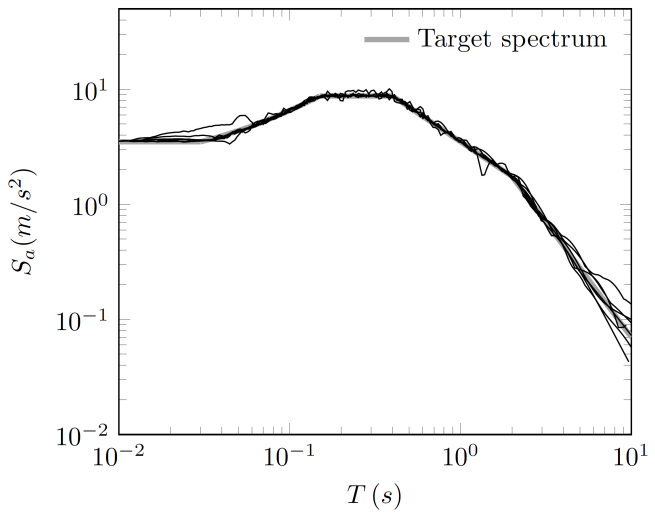

Figure 1: Response spectra of the horizontal components of the 7 synthetic accelerograms compared to the target response spectrum for a 5,000-year return period event according to the Eurocode 8 rules.

of Arias intensities:

$$I_a = \frac{\pi}{2g}\int_0^\tau [a_g(t)]^2\ \mathrm{d}t. \tag{2}$$

where τ is the duration of the accelerogram (s). The Arias intensities of each synthetic accelerogram generated is given in Table 3.

2.3. Dynamic analysis approach

The decoupled rigid sliding block model is used in the present study. The first step of this model consists in determining the yield acceleration $k_y\,g$. For a given block, the yield acceleration is the value of horizontal acceleration leading the block to its limit equilibrium. At that point, the effects of destabilizing actions, gravity and earthquake loading, are equal to the resisting forces from the shear strength mobilized along the slip surface. The shear strength is assumed to be bounded by a Mohr-Coulomb criterion. It is noteworthy that the yield acceleration depends only on the shear strength parameters and the geometry of the sliding mass. This parameter is independent of stiffness moduli, damping or ground motion parameters. When subjected to earthquake loading, the block starts to slide if the block acceleration exceeds the yield acceleration. Sliding continues until the relative velocity between the block and its base reaches zero. The double integration over time of the acceleration exceeding the yield acceleration gives the cumulative block displacement.

The shapes of the sliding surfaces are assumed to be

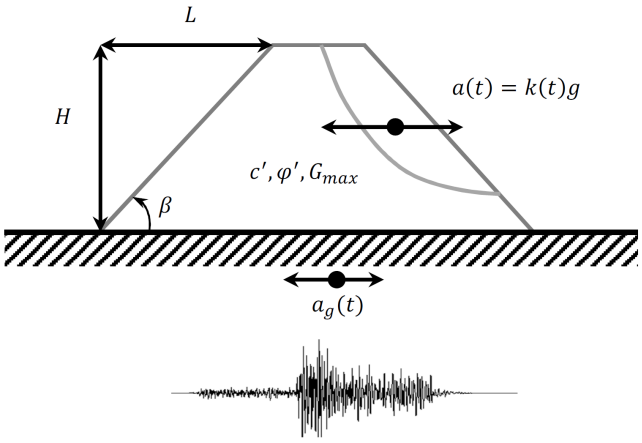

Figure 2: Geometrical, geotechnical and seismic loading parameters involved in the decoupled dynamic analysis approach.

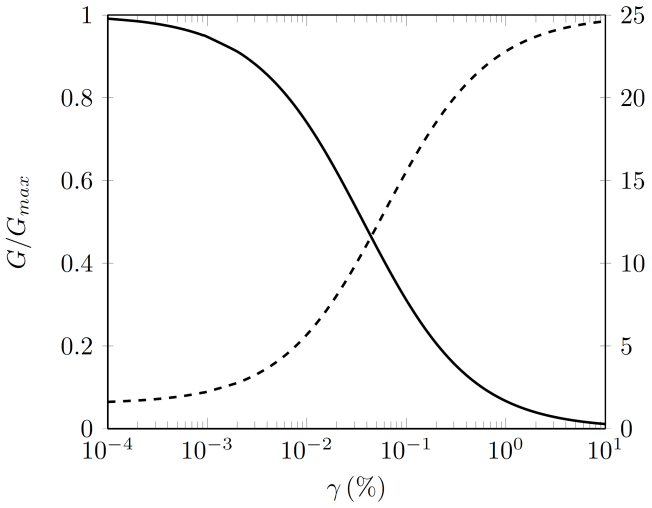

Figure 3: Shear modulus ratio G/G_{max} (solid line) and damping ratio ξ (dashed line) curves *versus* distorsion γ used in the linear equivalent method [37].

circular. The potential sliding of hundreds of blocks is calculated for each situation defined by a given set of geometrical, geotechnical and earthquake loading parameters. Shallow sliding blocks are not expected to significantly affect the geometry of the embankment and the safety level of the dam. Therefore, following the recommendations of OFEG [41], we only selected the blocks whose thickness was greater than 15% of the height of the embankment. The earthquake-induced displacement finally reported, which corresponds to the most critical situation, is the largest one obtained in the set of blocks considered.

The 2D response analyses of the dam were carried out using the finite element CAD software QUAKE/W GeoStudio [21] which performs seismic ground response analysis in the time domain. The seismic loading $a_g(t)$ was applied directly to the bedrock. The non-linear stress-strain soil behavior and the strain-dependent damping were taken into account through the linear equivalent procedure [51], in which the soil is modeled as a visco-elastic material. In the linear equivalent method, the linear analysis is solved repeatedly until the stiffness and the maximum shear strain response of each element satisfies the material relationship between the stiffness and the shear strain (Fig. 3). The FE analyses were carried out under plane strain conditions using quadrangular eight-noded elements with four-point Gaussian integration and a second-order polynomial interpolation for the displacements. To avoid numerical distortion of the propagating wave during the dynamic analysis, the maximum size of elements (Δl_{max}=1 m) was smaller than 1/6 of the wavelength associated with the highest frequency component of the input wave f_{max} [30]. A value of f_{max} = 20 Hz was fixed since negligible energy content is associated to higher frequencies (Fig. 1). Depending on the dimensions of the structure, the number of elements varies from 742 to 1434.

The acceleration-time history of each block was then calculated by integrating the local accelerations over the whole volume of each block. The integration time step was chosen equal to the time step of the accelerogram records (Δt=0.01s). This approach is therefore considered as a "decoupled" approach because the determination of the acceleration-time history of the blocks and the evaluation of the permanent displacements are performed sequentially.

3. Results

The calculations of earthquake-induced permanent displacements were performed for 33 different situations using the combinations of the geometric and geotechnical configurations listed in Table 2. Each configuration was subjected to the 7 accelerograms presented in Table 3. Finally, the permanent displacement analyses were performed on 231 simulations.

3.1. Pseudo-static analysis

The first step for any Newmark analysis is to perform a pseudo-static analysis in order to evaluate the yield coefficient k_y. The yield coefficient was determined for each block using the Morgenstern-Price limit equilibrium method [39].

Figure 4 shows the influence of the geometrical and geotechnical parameters on the yield coefficient k_y. It can be seen that k_y rises when the cohesion and internal friction angle increase (fig. 4a and 4b). These results agree with those of the extensive study published by Sarma and Bhave [49]. The yield coefficient increases linearly with ϕ' (Fig. 4b), whereas the correlation between k_y and c' is non-linear (Fig. 4a). The reason may be that the depth of the critical sliding surface increases as c' increases. Thus the mean normal stress acts on the sliding surface so that the contribution of c' on the total shear strength decreases.

Figure 4c shows a reduction of k_y when the embankment slope increases, which is trivial. It can be seen that k_y when H increases very slightly from 10 m to 20 m (Fig. 4d). This result demonstrates that the scale effect has little influence on the geometry of the critical sliding block and thus on the yield coefficient.

To carry out a rapid diagnosis, it can be interesting to link the static factor of safety, which is generally available, to the yield coefficient. In the simplest model of an infinite slope, the static factor of safety can be derived analytically [31, 47]. However, there is no analytical solution to the problem we are considering and the determination of k_y has to be performed numerically.

Figure 5 shows the static factor of safety as a function of the yield acceleration k_y, for the different slope configurations. As observed by Sarma and Bhave [49], the yield coefficient increases linearly with the static factor of safety. For each slope β, the data were fitted with a linear law that keeps a static factor of safety equal to one when k_y is zero. The following relationship was obtained :

$$k_y = \alpha \tan\beta \, (F - 1) \tag{3}$$

where α=0.80 is a regression coefficient ($R^2 = 0.97$), F is the static factor of safety and β the inclination of the slope. Equation 3 can be considered as an empirical way of evaluating the key parameter of our dynamic analysis, namely k_y, using the static factor of safety of the dam. It is worth noting that the value of α proposed here is very close to the value of α=0.78 which can be inferred from the data presented by Sarma and Bhave [49].

3.2. Decoupled analysis

Figure 6 displays all the permanent displacements estimated by the present Newmark analysis procedure as a function of the ratio between the critical acceleration $k_y\, g$ and the peak ground acceleration PGA. As the PGA remains constant for all the simulations, Figure 6 shows that the displacement decreases when k_y increases. This representation, commonly used in the literature, shows that permanent displacements occur even when $k_y g > PGA$. It can be seen that the dispersion of the calculated Newmark displacements increases with the acceleration ratio $k_y g > PGA$. It should be noted that the discontinuous grouping of the results into four clusters is due to the different geometrical and geotechnical configurations studied. Interestingly, the calculated Newmark displacements lie within the band of observational data published by Singh et al. [53].

Unlike complex stress-deformation modeling which requires significant computational efforts, decoupled dynamic procedures are suitable for performing parametric analysis. Figure 7 shows the influence of different input parameters on the prediction of earthquake-induced permanent displacements U. Each point corresponds to the calculation on one geometric and geotechnical configuration and one accelerogram.

Figures 7a and 7b show that the Newmark displacement U increases when the cohesion and the internal friction angle increase. For a given G_{max}, the differences of the Newmark displacements obtained for two Arias intensities increase as the shear strength parameters decrease. Reciprocally, for a given Arias intensity, the differences of the Newmark displacements obtained for two different G_{max} increase as the shear strength parameters decrease. These results suggest that the influence of ϕ' and c' increases as I_a increases or G_{max} decreases. The influence of the slope on the Newmark displacement is lower than that of the shear strength parameters (Fig. 7c). It can be seen that the influence of I_a increases as the slope increases and as G_{max} decreases. Figure 7d illustrates the effect of embankment height on the amplification phenomenon. It is well known that the amplification ratio $k_{max}g/PGA$ increases as the ratio between the depth of the sliding surface and the embankment height increases. Thus, for a given sliding block characterized by a yield coefficient k_y, the increase of H induces a decrease of the ratio k_y/k_{max} and consequently an increase of the Newmark displacement. It is also shown that the influence of I_a and G_{max} increase as H increases.

3.3. Comparison with existing methods

Our results were also compared to the existing methods presented in the introduction. k_{max} is determined for all the methods according to the approach developed by Makdisi and Seed to avoid the introduction of a bias in the comparison of simplified formulae. The sliding block giving the lowest yield coefficient was determined for each configuration. The Makdisi and Seed method was implemented for this block and two other blocks corresponding to twice and half the depth of the most critical block. Figure 8 shows that using the acceleration ratios k_y/k_{max} calculated by the Makdisi and Seed approach introduce uncertainties, but no systematical error with respect to the acceleration ratios k_y/k_{max} was obtained by our decoupled analyses.

The Hynes-Griffin and Franklin [25] method was used to estimate the mean values of the Newmark displacements. The Newmark displacements calculated by this method (U_{HGF}) are one order of magnitude lower than those obtained by the decoupled analysis, giving very unconservative results (Fig. 9a).

Newmark displacements were estimated according to the method developed by Sarma [48], assuming an average value for the coefficient $C = 0.85$. It can be seen that the displacements predicted by this method (U_S) also give unconservative results by one order of magnitude (Fig. 9b).

Our results are represented with the results obtained from the chart-based method developed by Makdisi and Seed [37]. It can be seen that the permanent displacement calculated by the Makdisi and Seed method (U_{MS}) is close to the values of the Newmark displacements estimated with the decoupled approach (Fig. 9c). However, they are

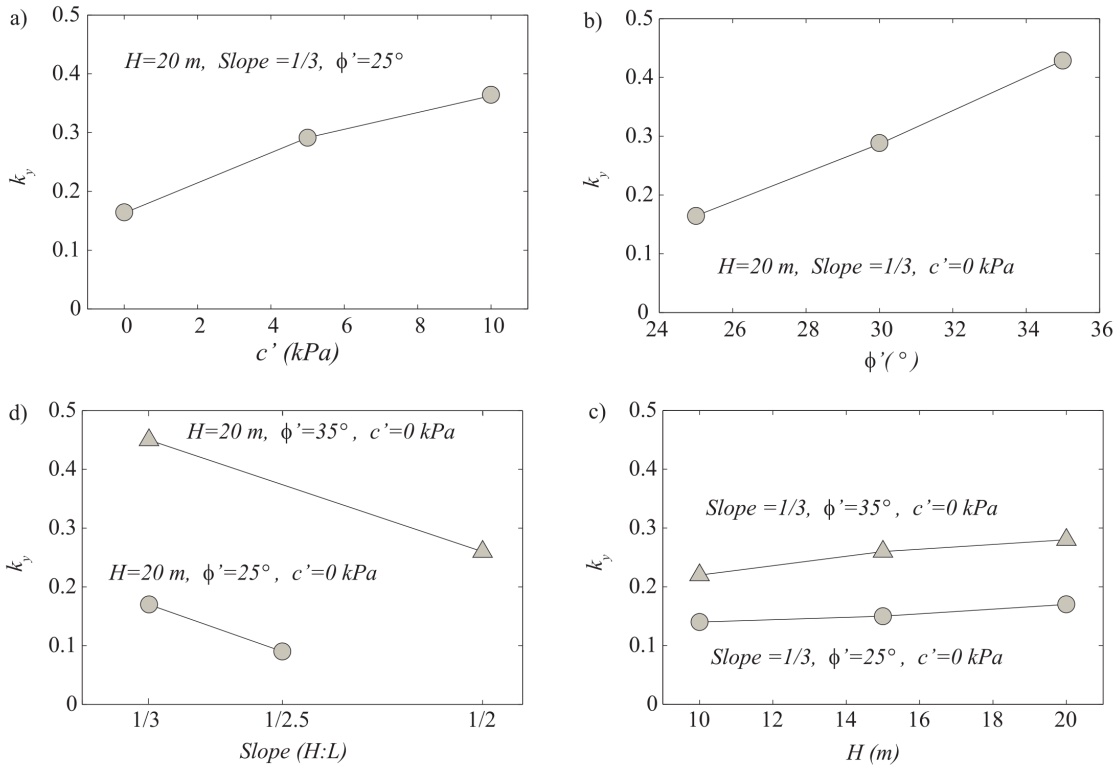

Figure 4: Yield coefficient k_y plotted *versus*: (a) cohesion c', (b) angle of internal friction Φ', (c) reservoir slope $H:L$, and (d) height H. In each case, G_{max}= 300 MPa and I_a= 0.9 m.s^{-2}.

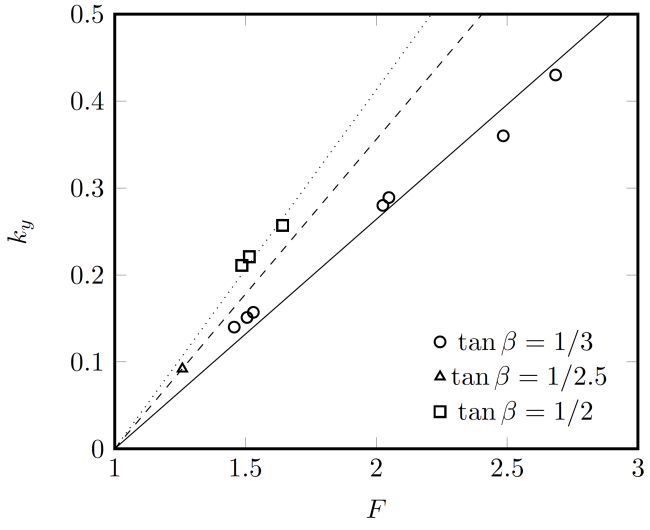

Figure 5: Static factor of safety plotted *versus* yield acceleration coefficient k_y. The curves represent the interpolation values given by Equation 3 for tanβ=1/2 (dotted), tanβ=1/2.5 (dashed) and tanβ=1/3 (solid).

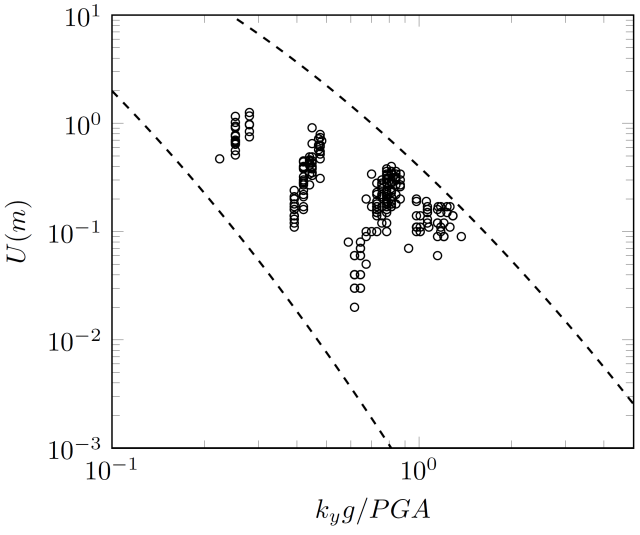

Figure 6: Calculated Newmark displacements as a function of the critical acceleration ratio $k_y g/PGA$. The dashed curves represent the boundaries of the observational data published by Singh et al. [53].

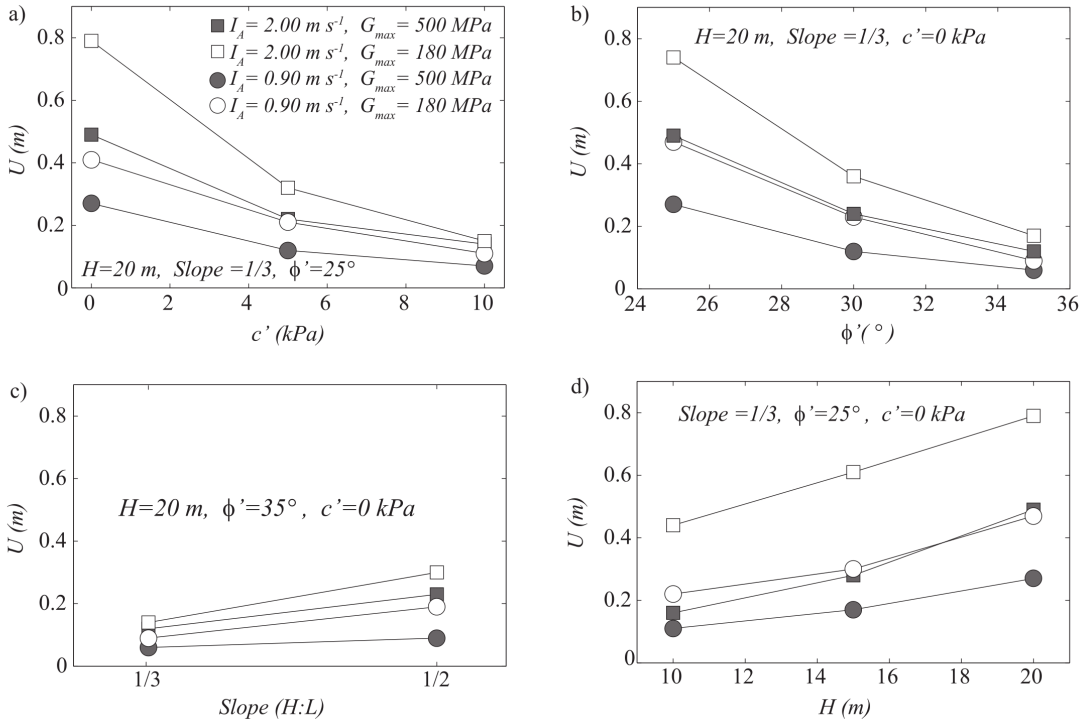

Figure 7: Plot of the estimated seismic displacement U *versus*: (a) cohesion c', (b) angle of internal friction Φ', (c) embankment slope, and (d) height H.

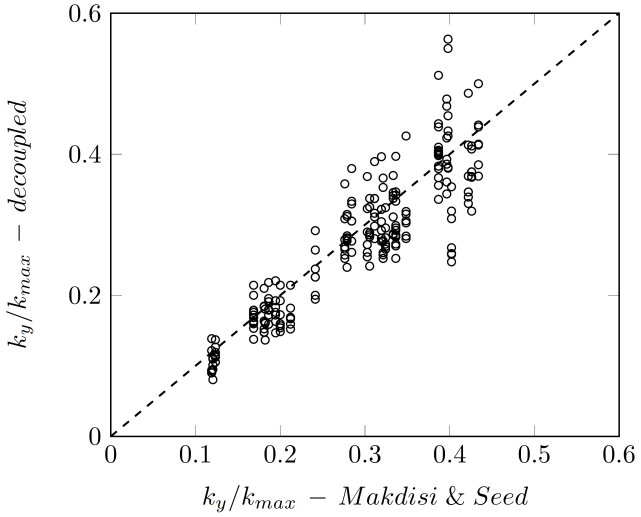

Figure 8: Comparison of the ratio between the yield coefficient and the peak acceleration coefficient k_y/k_{max} obtained by the Makdisi and Seed method and decoupled approach. The dashed line is the bisector line.

systematically smaller than those predicted by our simulations. This result is in accordance with Andrianopoulos et al. [3] who demonstrated that the chart developed by Makdisi and Seed is unconservative for $H \leq 20$ m. These differences may be due to different input ground motions used to calibrate the method. Indeed, the Makdisi and Seed method was calibrated for larger dams and a lower seismic energy content in the low frequencies ($T > 0.3\,s$).

The Newmark displacements were also estimated according to the Yegian et al. [60] method, assuming a number of equivalent cycles $N_{eq} = 5.5$. Several investigators [18] have shown that parameter T_m is almost constant over the height of the dam, and is close to its first fundamental period T_1. Therefore, from the practical point of view, T_m could be substituted by T_1 in the expression of the normalized Newmark displacement. Figure 9d shows that this approach gives good results for large values of displacements ($U \approx 0.5 - 1.0\,m$). However, the conservativeness of this method decreases as the displacement decreases. Therefore this approach is not conservative for $U \leq 0.5\,m$.

The method proposed by Bray and Travasarou [9] gives Newmark displacements (U_{BT}) close to the values obtained with the decoupled approach (Figure 9e). However, they generally remain smaller than those predicted is our simulations.The formula proposed by Jibson [27] is clearly unconservative for values of displacements smaller than $U \leq 0.5\,m$ (Figure 9f).

To conclude, although the results of our numerical anal-

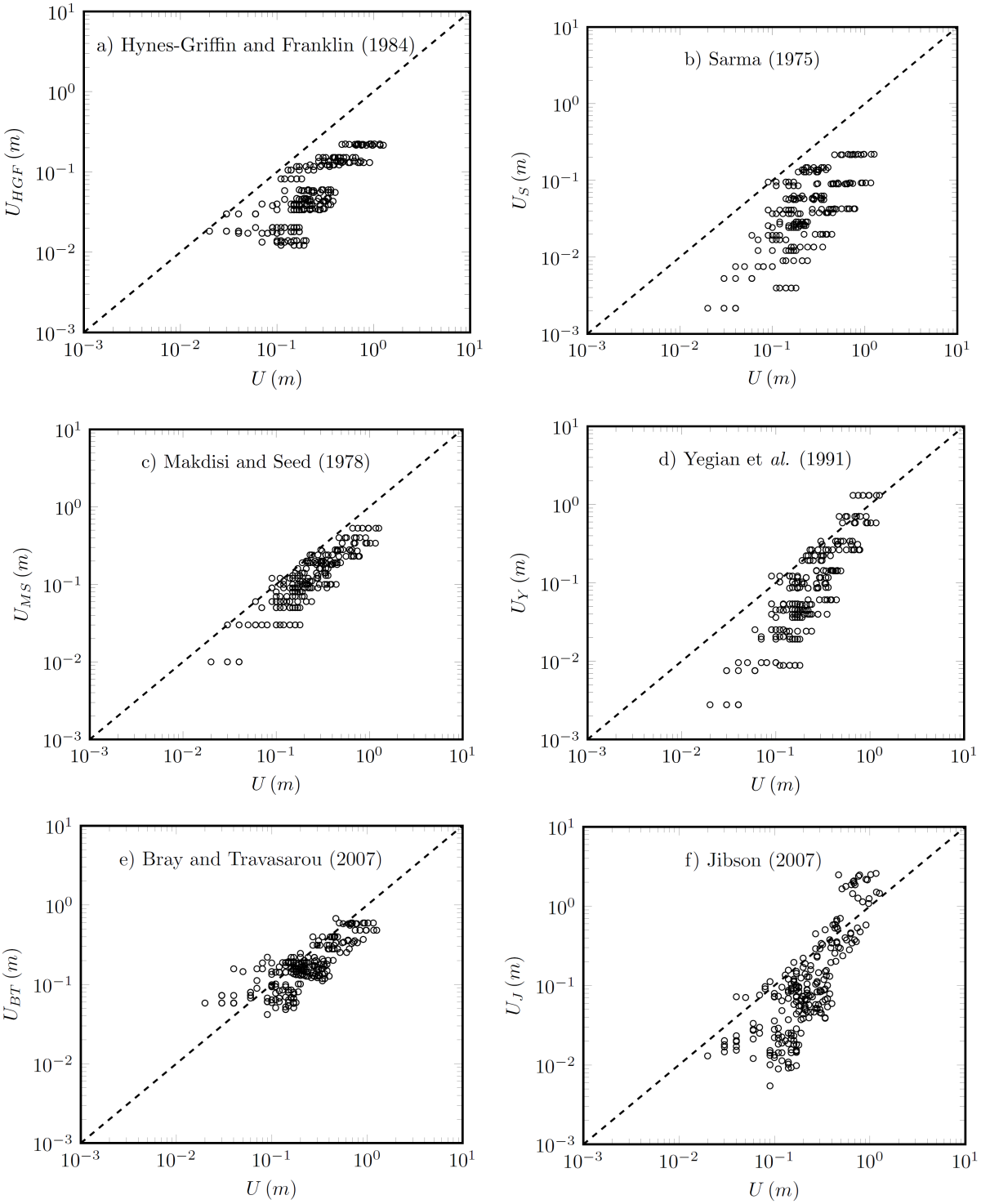

Figure 9: Comparison between the Newmark displacements calculated according to the rigorous decoupled approach and the existing simplified approaches.

ysis are consistent with those obtained from other existing simplified models, none of them provides a conservative and satisfactory framework for the evaluation of Newmark displacements of mountain reservoirs. Therefore the development of a simplified method adapted to the case of mountain reservoirs requires the establishment of a new formulation.

4. Predictive model

The aim of the present study is to supply a practical tool for assessing the seismic performance of large mountain reservoirs. Thus it is desirable to identify variables that minimize the variability in the correlation with the Newmark displacement, that are independent from each other, and that are easily accessible without performing complex dynamic computations. This will lead to a drastic reduction of the time, computational efforts and cost of assessing the seismic performance of large mountain reservoirs.

4.1. Selection of normalization variables

The magnitude of the earthquake-induced seismic displacement of an embankment depends on the characteristics of the ground motion and the embankment properties.

The Newmark displacement should be normalized by a parameter representative of the intensity of the ground motion. No unique ground motion variable can be expected to be capable of capturing all the aspects influencing earthquake-induced ground motion (magnitude, frequency content, duration, etc.). Thus the goal is to identify the optimal variable that is as efficient and sufficient as possible. In the existing methods, the variable representing the ground motion intensity is proportional to PGA. However, PGA is already taken into account *via* the yield acceleration ratio $k_y g/PGA$. Moreover, PGA is not an adequate representation of the intensity of the ground motion as it only measures a single point in an acceleration time history. On the contrary, the Arias intensity (Eq. 2) is a measure of earthquake intensity related to the energy content of the signal recorded. It is a cumulative energy function which represents the total acceleration content of the record rather than just the peak value. It is believed that it provides a more complete characterization of the shaking content than the peak ground acceleration [26]. Moreover, it has been demonstrated to be a pertinent ingredient for the assessment of slope seismic performance [58, 26, 23, 47, 56, 27, 32, 50, 24, 34].

It is well known that seismic displacement also depends on the vibratory characteristics of the embankments [2, 20, 13]. It is governed by the embankment height and stiffness characteristics and is usually dominated by the first fundamental period of the dam [52, 19].It can be approximated by the following expression [2]:

$$T_1 = \frac{2\pi}{2.4}\frac{H}{\sqrt{G_{max}/\rho}} \tag{4}$$

Where H is the embankment height, G_{max} is the maximum shear modulus and ρ is the density of the embankment. It is noteworthy that this parameter group combines two of the most influential parameters identified in the sensitivity analysis performed earlier: H and G_{max}.

Figures 10a and b represent Newmark displacements U for all the data as a function of I_a and T_1 respectively. These graphs gather all the results of the 231 simulations. It can be seen that U increases as I_a and T_1 increase. Indeed, the regression curve on I_a shows that U is multiplied by 2 as I_a increases from 0.9 to 2.0. The regression curve on T_1 shows that U is multiplied by 10 as T_1 increases from 0.05 s to 0.18 s. The range of calculated Newmark displacement is from 2-3 cm to more than 100 cm. The upper and lower bounds reproduces well the upper bounds obtained in other studies [47, 9, 50, 24] for the same range of yield accelerations, Arias intensities and mean periods. This preliminary analysis suggests the use of the following non-dimensionalized displacement:

$$U^* = \frac{U}{I_a\, T_1} \tag{5}$$

4.2. Functional form for predicting displacements

Contrary to the normalization variables, which are intrinsic parameters of the ground motion and the structure, the functional $\mathcal{G}$ (Eq. 1) should describe the mechanical interaction between the structure and the seismic action. It is well known that the most influential parameter in the Newmark displacement estimation is the yield coefficient k_y. It can be seen in Fig. 6 that the Newmark displacement is multiplied by 10 and the yield coefficient is divided by 5. The coefficient k_y can be obtained by a pseudo-static limit equilibrium analysis or by the empirical relationship developed previously (Eq. 3) from the static factor of safety.

The amplification phenomenon is related to coupling effects between the frequency content of the seismic action and the vibratory behavior of the structure. Following earlier works [9, 57], the spectral acceleration at a degraded period equal to 1.5 times the initial fundamental period of the structure $S_a(1.5\,T_1)$ was found to be significantly correlated to the Newmark displacement (Fig. 10c). The use of the degraded fundamental period is expected to capture the average stiffness reduction of the structure occurring during the seismic loading. The regression parameters were determined by minimizing the coefficient of determination between the curve and the scatter plot. Our analyses led to the following functional form for estimating earthquake-induced displacements:

$$\ln U^* = -0.56 - 2.23\frac{k_y g}{PGA} + 2.8\ln\frac{S_a(1.5\,T_1)}{PGA} \tag{6}$$

The comparison between the Newmark displacements calculated by the decoupled approach (U) and the displacements predicted by Eq. 6 ($U_{predicted}$) is represented in

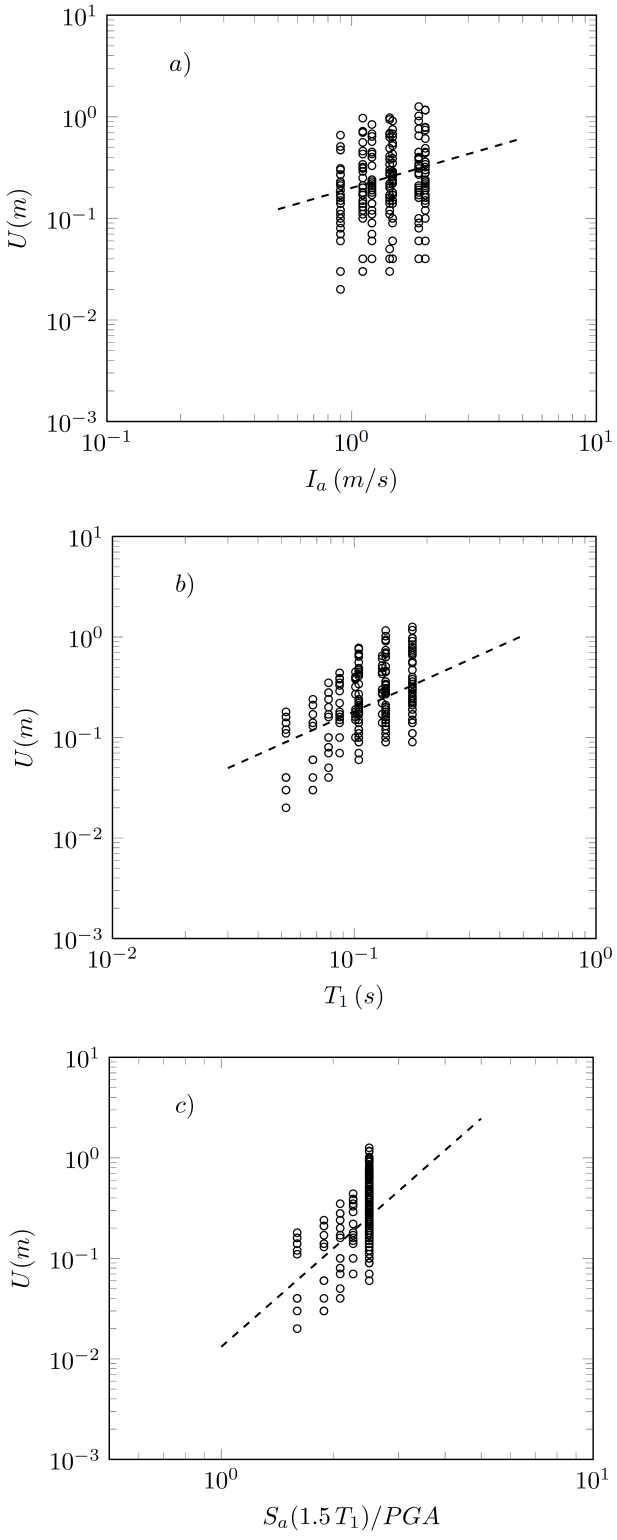

Figure 10: Displacement predicted by the present plotted model *versus*: (a) Arias intensity, (b) first fundamental period of the dam (s) and (c) the spectral acceleration at the degraded period $1.5\,T_1$. The linear regression curves are represented by the dashed lines.

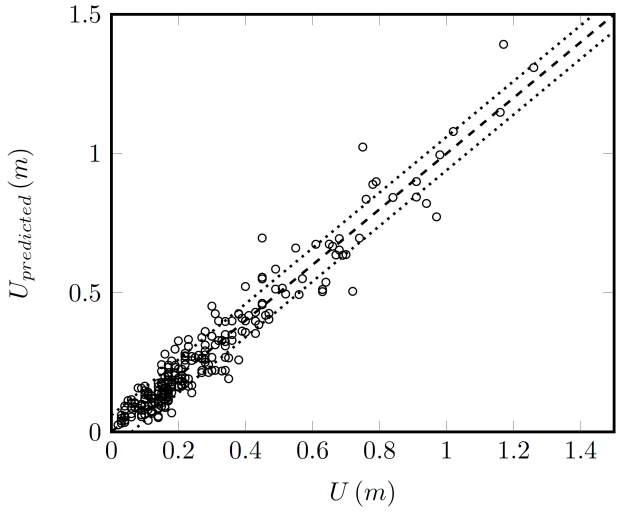

Figure 11: Newmark displacements predicted by the simplified method (Eq. 6) *versus* Newmark displacement calculated by the decoupled approach (circles). The dotted line represents the displacement values ± the standard deviation σ.

Fig. 11. The standard error on the Newmark displacement estimate is equal to 0.063 m and the coefficient of determination is equal to $R^2 = 0.93$.

The asymptotic behavior can be analyzed to verify the consistency of the model. For a given value of $S_a(1.5\,T_1)$ and $k_y\,g >> PGA$, the permanent displacement tends to zero, except in the case of an infinitely flexible embankment. When $k_y\,g << PGA$, we obtain $U \propto I_a T_1$. This means that in the case of very small shear strength properties, the permanent displacement only depends on the intensity of the ground motion and the vibratory characteristics of the structure. In particular, it is interesting to note that for a very stiff embankment ($T_1 \approx 0$) we obtain $U \approx 0$, which is consistent. However, practical experience shows that the amplification ratio $k_{max}\,g/PGA$ should not exceed 4.5 [25]. Thus, for critical ratios $k_y\,g/PGA \leq 1/4.5 \approx 0.2$, mechanisms leading to severe loss of shear strength such as liquefaction should be considered.

4.3. Comparison to field data

Several authors showed that Newmark sliding-blocks analyses could be used successfully to assess earthquake induced permanent displacements of earth dams [52, 28, 13, 44]. The predictive ability of the model developed in the present study can also be compared to actual post-seismic observations. A selection of field data, which all correspond to dams and landfills founded on rock or soft rock, are presented in Table 4. Most of the earthquake and structure parameters were taken from Bray and Travasarou [9] and Singh et al. [53]. Additional material was found in Harder et al. [22] for the dams exposed to the Loma Prieta earthquake, and in other references for the La Villita dam [59] and Cogswell dam [6]. The Arias

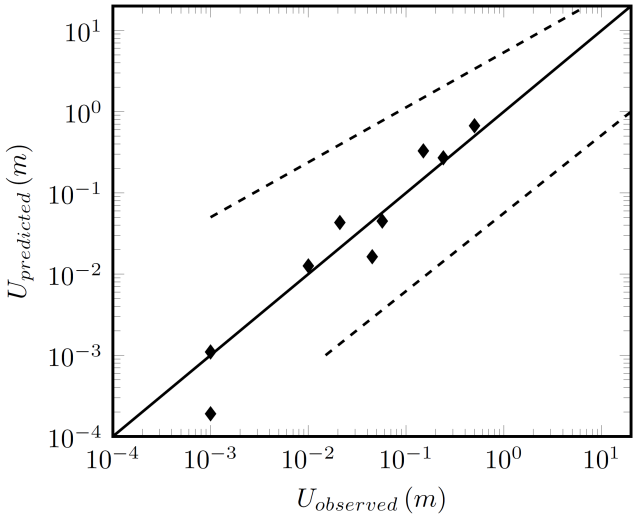

Figure 12: Observed *versus* predicted displacements for the proposed formula (Eq. 6) and the range of results obtained from field observations based regression models (dashed lines) [53, 57].

intensities were determined from the empirical attenuation relationships proposed by Travasarou et al. [56].

For the cases in which the permanent displacements are minor (less than 2 cm), the method proposed provides consistent estimates (Table 4). For cases with moderate observed displacements, the post-seismic permanent displacements measured *in situ* remain within the range of the Newmark displacement values calculated by the decoupled approach. Moreover, the error made when using the simplified method estimate does not exceed 0.18 m for every observation.

Figure 12 shows that the field observation points are located above the bisector line for observed displacements larger than 0.1 m, suggesting that the proposed simplified approach is conservative. Moreover, it can be seen that the scatter of our results is smaller than the scatter of those obtained from field observation-based regression models [53, 57].

Therefore, our predictive model seems to give robust estimates of permanent displacements, even for broader typologies of seismic loadings and structure than those used for model calibration. The consideration of a single value of PGA and one type of spectrum does not seem to attenuate the generality of our formulation. Indeed, the variability of the seismic loading, the range of Arias intensities considered, and the geotechnical configurations in terms of the natural periods and yield accelerations generated, allowed us to scan a wide spectrum of design situations.

4.4. Illustrative example

To illustrate the use of the approach proposed, the seismic performance of the Vars Dam was analyzed. The Vars Dam is a 21 m high mountain reservoir located in the southern Alps (Fig. 13). It was built in 2010 by cut

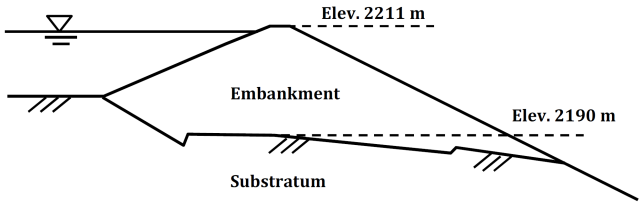

Figure 13: Representative cross section of the Vars dam.

and fill and retains 125,000 cubic meters of water. The current European regulations require that its good performance must be checked for a seismic hazard corresponding to a return period T = 2,500 years characterized by $PGA = 2.8m/s^2$. A set of 10 accelerograms was generated following the same methodology as the previous analyses performed for a return period T = 5,000 years (Fig.14).

The Multichannel Analysis of Surface Wave (MASW) seismic method was used to measure shear wave velocity and evaluate material properties. The representative shear wave velocity of the embankment was evaluated as $V_s = 450\,m/s$ corresponding to a maximum shear modulus $G_{max} = 480\,MPa$. The decoupled analysis performed on the representative cross section of the dam using a collection of specific synthetic accelerograms (different from those in Table 3) gave Newmark displacements $U = 3.0 - 13.0cm$.

The yield acceleration was estimated from a pseudo static analysis as $k_y = 3.8\,m/s^2$. The first fundamental period of the dam was estimated as equal to $T_1 = 0.12\,s$. The response spectrum corresponding to the regulatory requirements yield was $S_a(1.5T_1) = 7.0\,m/s^2$. For the PGA considered, the range of Arias intensities was evaluated as $I_a = 0.4 - 2.9$ [35]. Finally, the Newmark displacement estimated from the proposed simplified formula (Eq. 6) gives $U = 1.7 - 12.5\,cm$.

The Newmark displacements calculated from the decoupled analysis lie within the range of the Newmark displacements calculated from the simplified approach. Therefore, it was considered that the predictive equation developed previously was successful in estimating the performance of the Vars dam, even if the ground motion characteristics were different from those used to calibrate the predictive equation of the Newmark displacement. This illustrative example confirms that the integration of spectral parameters in the formulation of the simplified method extended its range of validity beyond the 5,000-year return period for earthquakes.

5. Conclusion

A Newmark analysis was implemented to determine the earthquake-induced permanent displacements in homogeneous mountain reservoirs situated in the French-Italian

Dam	Earthquake	k_y	T_1 (s)	PGA (m/s^2)	I_a (m/s)	$S_a(1.5T_1)$ (m/s^2)	$U_{observed}$ (m)	$U_{predicted}$ (m)
Austrian Dam	LP	0.14	0.33	0.60	1.70	0.94	0.50	0.67
Lexington Dam	LP	0.11	0.31	0.40	1.05	0.61	0.15	0.33
Anderson Dam	LP	0.12	1.08	0.13	1.14	0.10	0.021	0.043
Guadalupe Landfill	LP	0.20	0.64	0.42	0.90	0.21	0.045	0.016
Pacheco Pass Landfill	LP	0.30	0.76	0.20	0.30	0.12	≤ 0.01	0.001
La Villita Dam	MI	0.20	0.60	0.10	0.40	0.33	0.057	0.046
Chabot Dam	SF	0.14	0.55	0.56	0.60	0.26	≤ 0.05	0.013
Cogswell Dam	WN	0.12	0.69	0.06	0.13	0.04	≤ 0.01	0.0002
Chiquita Canyon Landfill	NR	0.09	0.64	0.33	1.15	0.35	0.24	0.27

LP : Loma Prieta (October 17, 1989), M_w=7.0
MI : Michaocan (September 19, 1985), M_w=8.1
NR : Northridge (January 17, 1994), M_w=6.7
SF : San Francisco (April 18, 1906), M_w=8.3
WN : Whittier Narrows (October 1, 1987), M_w=6.0

Table 4: Comparison of calculated Newmark displacements *via* the proposed predicted equation (Eq. 6) with post-seismic observed displacements.

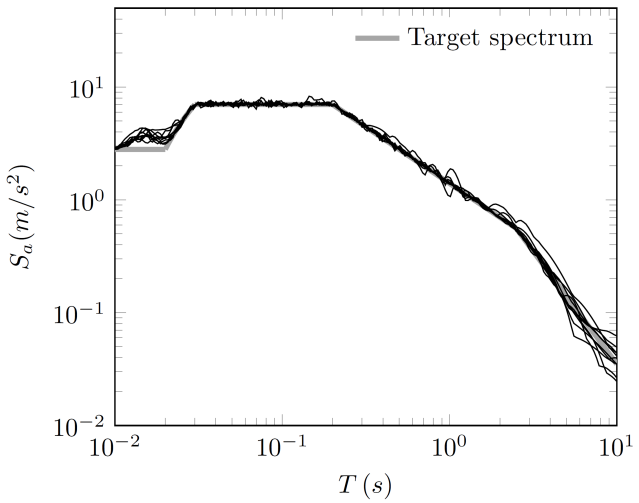

Figure 14: Response spectra of the horizontal components of the 10 synthetic accelerograms compared to the target response spectrum for a 2,500-year return period event according to the Eurocode 8 rules.

Alpine cross-border area. Our numerical procedure consisted of a decoupled dynamic analysis based on sequential calculations involving a linear equivalent approach, followed by a Newmark sliding block analysis. The numerical results obtained from 231 simulations were in accordance with field data and provided consistent results in comparison to other existing simplified methods. A sensitivity analysis was performed to estimate the influence of soil cohesion, internal friction angle, shear modulus, and embankment height and slope, on both the permanent displacement and the yield coefficient.

The results of simulations were used to establish a regression law to predict seismic displacements on the basis of the input parameters usually available, namely in terms of critical acceleration ratio, Arias intensity, acceleration response spectrum and the fundamental period of the structure (Eqs. 5 and 6). An empirical relationship was also established to obtain k_y directly from the static factor of safety (Eq. 3). The comparison of our results with existing methods and *in situ* observations showed that the validity of this formulation probably goes beyond the scope of alpine mountain reservoirs.

Acknowledgments

The present study has been developed within the European project RISBA (*Risque des barrages*, Interreg Alcotra 2007-2013 program N^{o}187) in collaboration with Piedmont and Aosta Valley Regions, Italy. The authors wish to thank Alain Gérard (Irstea) posthumously for his anonymous but crucial contributions to this research work and others.

References

[1] Akkar, S., Sandikkaya, M., Senyurt, M., Azari Sisi, A., Ay, B., Traversa, P., Douglas, J., Cotton, F., Luzi, L., Hernandez, B.,

S., G., 2014. Reference database for seismic ground-motion in europe (resorce). Bulletin of Earthquake Engineering 12, 311–339.

[2] Ambraseys, N., Sarma, S.K., 1967. The response of earth dams to strong earthquakes. Géotechnique 17, 181–213.

[3] Andrianopoulos, K.I., Papadimitriou, A.G., Bouckovalas, G., Karamitros, D., 2014. Insight into the seismic response of earth dams with an emphasis on seismic coefficient estimation. Computers and Geotechnics 55, 195–210.

[4] Bard, P.Y., Causse, M., 2015. Generation of synthetic accelerograms for alpine dams. Technical Report. ISTerre, Grenoble, France.

[5] Betbeder-Matibet, J., 2008. Seismic Engineering. Wiley.

[6] Boulanger, R., Seed, R., Bray, J., 1993. Investigation of the response of Cogswell dam in the Whittier Narrows earthquake of october 1,1987. Technical Report. Department of Civil Engineering, University of California, Berkeley, California.

[7] Bozbey, I., Gundogdu, O., 2011. A methodology to select seismic coefficient based on upper bound Newmark displacement using earthquake records from Turkey. Soil Dynamics and Earthquake Engineering 31, 440–451.

[8] Bray, D., 2007. Earthquake Geotechnical Engineering. Springer. chapter Simplified seismic slope displacement procedures. pp. 327–354.

[9] Bray, D., Travasarou, T., 2007. Simplified procedure for estimating earthquake-induced deviatoric slope displacements. Journal of Geotechnical and Geoenvironmental Engineering 133, 381–392.

[10] Bray, D., Travasarou, T., 2009. Pseudostatic coefficient for use in simplified slope stability evaluation. Journal of Geotechnical and Geoenvironmental Engineering 135(9), 1336–1340.

[11] Bray, J.D., Rathje, E.M., Augello, A.J., Merry, S.M., 1998. Simplified seismic design procedures for geosynthetic-lined, solid waste landfills. Geosynthetics International 5(1-2), 203–235.

[12] Cai, Z., Bathurst, R.J., 1996. Deterministic sliding block methods for estimating seismic ddisplacement of earth structures. Soil Dynamics and Earthquake Engineering 15, 255–268.

[13] Cascone, E., Rampello, S., 2003. Decoupled seismic analysis of an earth dam. Soil Dynamics and Earthquake Engineering 23, 349–365.

[14] Clough, R.W., Chopra, A.K., 1966. Earthquake stress analysis in earth dams. ASCE Journal of the Engineering Mechanics Division 92, 197–211.

[15] Deyanova, M., Lai, C.G., Martinelli, M., 2016. Displacement-based parametric study on the seismic response of gravity earth-retaining walls. Soil Dynamics and Earthquake Engineering 80, 210–224.

[16] Eurocode 8, 2004. Design of structures for earthquake resistance - part 1: General rules, seismic actions and rules for buildings.

[17] Gasparini, D.A., Vanmarcke, E.H., 1976. Simulated earthquakes compatible with prescribed response spectra. Technical Report. Massachusetts Institute of Technology, Publication No. R76-4, Cambridge, Massachusetts.

[18] Gazetas, G., 1987. Seismic response of earth dams: Some recent developments. Soil Dynamics and Earthquake Engineering 6(1), 2–47.

[19] Gazetas, G., Doukoulas, P., 1992. Seismic analysis and design of rockfill dams: state-of-the-art. Soil Dynamics and Earthquake Engineering 11, 27–61.

[20] Gazetas, G., Uddin, N., 1994. Permanent deformation on pre-existing sliding surface in dams. Journal of Geotechnical Engineering Division, ASCE 120(11), 2041–2061.

[21] GeoSlope International Ltd., 2004. Geostudio a product suite for geotechnical modeling.

[22] Harder, L., Bray, J., Volpe, R., Rodda, K., 1998. Performance of earth dams during the Loma Prieta Earthquake. Technical Report. U.S. Geological Survey professional paper 1552-D.

[23] Harp, E., Wilson, R., 1995. Shaking intensity for rock falls and slides: evidence from 1987 whittier narrows and superstition hills earthquake strong-motion records. Bulletin of the Seismological Society of American 85(6), 1739–1757.

[24] Hsieh, S., Lee, C., 2011. Empirical estimation of the Newmark displacement from the Arias intensity and critical acceleration. Engineering Geology 122, 34–42.

[25] Hynes-Griffin, M.E., Franklin, A.G., 1984. Rationalizing the seismic coefficient method, Misc. Paper GL-84-13. Technical Report. U.S. Army Waterway Experiment Station, Vicksburg, Mississipi.

[26] Jibson, R.W., 1993. Predicting earthquake-induced landslide displacements using Newmark's sliding block analysis. Transportation Research Record 1411, 9–17.

[27] Jibson, R.W., 2007. Regression models for estimating coseismic landslide displacement. Engineering Geology 91, 209–218.

[28] Kramer, L.K., Smith, M.W., 1997. Modified Newmark model for seismic displacement of compliant slopes. Journal of Geotechnical and Geoenvironmental Engineering 123(7), 635–644.

[29] Kramer, S.L., 1996. Geotechnical Earthquake Engineering. Prentice Hall, Upper Saddle River, N.J.

[30] Kulhmeyer, R., Lysmer, J., 1973. Finite element method accuracy for wave propagation problems. Journal of Soil Mechanics and Foundation Division, ASCE 99(5), 421–427.

[31] Lambe, T., Whitman, R., 1983. Soil Mechanics - Dynamic analysis of a slope. Wiley, Wilson, R.C., Keefer, D.K., New York. p. 553.

[32] Lee, C., Huang, C., Lee, J., Pan, K., Lin, M., Dong, J., 2008. Statistical approach to earthquake-induced landslide susceptibility. Engineering Geology 100, 43–58.

[33] Lee, J., Ahn, J., Park, D., 2015. Prediction of seismic displacement of drymountain slopes composed of a soft thin uniform layer. Soil Dynamics and Earthquake Engineering 79, 5–16.

[34] Lenti, L., Martino, S., 2012. The interaction of seismic waves with step-like slopes and its influence on landslide movements. Engineering Geology 126, 19–36.

[35] Lenti, L., Martino, S., Rinaldis, D., 2012. Lema des equivalent signals derived from the accelerometric records of the european database, in: 15th world conference on earthquake engineering, Lisboa, pp. 813–846.

[36] Lin, J.S., Whitman, R.V., 1983. Decoupling approximation to the evaluation of earthquake-induced plastic slip in earth dams. Earthquake Engineering and Structural Dynamics 11, 667–678.

[37] Makdisi, F.I., Seed, H.B., 1978. Simplified procedure for estimating earth dam and embankment earthquake-induced deformations. Journal of Geotechnical Engineering Division, ASCE 104(GT7), 849–867.

[38] Meehan, C.L., Vahedifard, F., 2013. Evaluation of simplified methods for predicting earthquake-induced slope displacement in earth dams and embankments. Engineering Geology 152, 180–193.

[39] Morgenstern, N., Price, V., 1965. The analysis of the stability of general slip surfaces. Géotechnique 15, 70–93.

[40] Newmark, N.M., 1965. Effects of earthquakes on dams and embankments. Geotechnique 15, 139–159.

[41] OFEG, 2003. Dam safety - Base document for the verification of dams subjected to earthquakes. Technical Report. OFEG, serie Eaux, version 1.2.

[42] Papadimitriou, A.G., Bouckovalas, G.D., Andrianopoulos, K.I., 2014. Methodology for estimating seismic coefficient for performance-based design of earth dams and tall embankments. Soil Dynamics and Earthquake Engineering 56, 57–73.

[43] Peyras, L., Mériaux, P. (Eds.), 2009. Retenues d'altitudes. Quae.

[44] Pradel, D.P., Smith, P.M., Stewart, J.P., Raad, G., 2005. Case history of landslide movement during the northridge earthquake. Journal of Geotechnical and Geoenvironmental Engineering 131(11), 1360–1369.

[45] Rathje, E.M., Antonakos, G., 2011. A unified model predicting earthquake-induced sliding displacements of rigid and flexible slopes. Engineering Geology 122, 51–60.

[46] Rathje, E.M., Bray, J.D., 1999. An examination of simplified earthquake-induced displacement pprocedure for earth structures. Canadian Geotechnical Journal 36, 72–87.

[47] Romeo, R., 2000. Siesmically induced landslide displacements: a predictive model. Engineering Geology 58, 337–351.
[48] Sarma, S.K., 1975. Seismic stability of earth dams and embankments. Géotechnique 25(4), 743–761.
[49] Sarma, S.K., Bhave, M.V., 1994. Critical acceleration versus static factor of safety in stability analysis of earth dams and embankments. Geotechnique 24(4), 661–665.
[50] Saygili, G., Rathje, E.M., 2008. Empirical predictive models for earthquake-induced sliding displacements of slopes. Journal of Geotechnical and Geoenvironmental Engineering 134(6), 790–803.
[51] Seed, H.B., Idriss, I.M., 1970. Soil moduli and damping factors for dynamic response analysis, Report No. EERC 70-10. Technical Report. University of California, Berkeley.
[52] Seed, H.B., Makdisi, I.F., De Alba, P., 1978. Performance of earth dams during earthquakes. Journal of Geotechnical Engineering Division, ASCE 104(7), 967–994.
[53] Singh, R., Roy, D., Das, D., 2007. A correlation for permanent earthquake-induced deformation of earth embankments. Engineering Geology 90, 174–185.
[54] Song, J., Gao, G., Rodriguez-Marek, A., Rathje, E.M., 2016. Seismic assessment of the rigid sliding displacements caused by pulse motions. Soil Dynamics and Earthquake Engineering 82, 1–10.
[55] Terzaghi, K., 1950. Mechanisms of landslides. Geological Society of America. chapter Application of Geology to Engineering practice. pp. 83–123.
[56] Travasarou, T., Bray, D., Abrahamson, A.N., 2003. Emprirical attenuation relationship for Arias intensity. Earthquake Engineering and Structural Dynamics 32, 1133–1155.
[57] Vahedifard, F., Meehan, C.L., 2011. A multi-parameter correlation for predicting the seismic displacement of an earth dam or embankment. Geotechnical and Geological Engineering 29, 1023–1034.
[58] Wilson, R., Keefer, D., 1983. Dynamic analysis of a slope failure from the 6 august 1979 coyote lake, california, earthquake. Bulletin of the Seismological Society of America 73, 863–877.
[59] Yan, L., 1991. Seismic deformation of earth dams: a simplified method. Technical Report. California Institute of Technology.
[60] Yegian, M., Marciano, E., Ghahraman, V., 1991. Earthquake-induced permanent deformations: probabilistic approach. Journal of Geotechnical Engineering 117(1), 35–50.